PNAS RESEARCH ARTICLE | ANTHROPOLOGY

Trabecular bone ontogeny tracks neural development and life history among humans and non-human primates

Jaap P. P. Saers[a,1], Adam D. Gordon[b], Timothy M. Ryan[c], and Jay T. Stock[a,d]

Edited by Clark Larsen, The Ohio State University, Columbus, OH; received May 24, 2022; accepted October 27, 2022

Trabecular bone—the spongy bone inside marrow cavities—adapts to its mechanical environment during growth and development. Trabecular structure can therefore be interpreted as a functional record of locomotor behavior in extinct vertebrates. In this paper, we expand upon traditional links between form and function by situating ontogenetic trajectories of trabecular bone in four primate species into the broader developmental context of neural development, locomotor control, and ultimately life history. Our aim is to show that trabecular bone structure provides insights into ontogenetic variation in locomotor loading conditions as the product of interactions between increases in body mass and neuromuscular maturation. Our results demonstrate that age-related changes in trabecular bone volume fraction (BV/TV) are strongly and linearly associated with ontogenetic changes in locomotor kinetics. Age-related variation in locomotor kinetics and BV/TV is in turn strongly associated with brain and body size growth in all species. These results imply that age-related variation in BV/TV is a strong proxy for both locomotor kinetics and neuromuscular maturation. Finally, we show that distinct changes in the slope of age-related variation in bone volume fraction correspond to the age of the onset of locomotion and the age of locomotor maturity. Our findings compliment previous studies linking bone development to locomotor mechanics by providing a fundamental link to brain development and life history. This implies that trabecular structure of fossil subadults can be a proxy for the rate of neuromuscular maturation and major life history events like locomotor onset and the achievement of adult-like locomotor repertoires.

trabecular bone | hominin | ontogeny | bone functional adaptation | locomotion

Significance

Trabecular (spongy) bone can dynamically change its structure in response to its mechanical environment during ontogeny. In paleoanthropology, trabecular bone is used to reconstruct the locomotor behavior of extinct hominins. We show that trabecular bone can illuminate other major unanswered questions in the field such as the evolution of neuromuscular developmental patterns and life history. The evolution of neural development is difficult to track because of the fragmentary nature of cranial fossils and absence of internal neural architecture. Here, we demonstrate fundamental relationships between trabecular bone morphology, locomotor development, and patterns of neural development in humans and other primates, providing a novel method to integrate neural development with skeletal development and major life history events in fossil taxa.

Bone morphology is partially determined by genetic processes regulating growth and development and partially by bone cells adapting to their mechanical environment (1–3). The structure of spongy (trabecular) bone found inside bones is thought to be particularly responsive to mechanical stimuli, superimposed upon an organism's developmental trajectory which may locally vary in degree of canalization (3–8). This concept is referred to as bone functional adaptation. The link between mechanical loading and the three-dimensional structure of trabecular bone allows locomotor and postural behavior to be reconstructed in fossil taxa (8–15). Alterations to ontogenetic trajectories are the principal ways in which evolutionary changes in life history and morphology occur (16–18). Unsurprisingly then, researchers are increasingly interested in the ontogeny of trabecular bone structure to infer the development of gait and posture in extinct species (19–23). In this paper, we build on previous studies linking locomotor ontogeny to trabecular bone morphology by placing it into the broader developmental context of neural development, locomotor control, and ultimately life history. We aim to demonstrate the fundamental links between brain development and the life history strategies associated with the speed of neural development and locomotor control, on the one hand, and age-related variation in locomotor loading and trabecular bone structure on the other. As such, we propose that ontogenetic variation in trabecular bone structure contains novel information regarding the rate of neuromuscular maturation and the timing of major life history events such as the onset of locomotion in fossil taxa.

Mammalian locomotion usually develops in a stereotypical sequence of events that dramatically changes how skeletons are loaded (24–26). Changes in loading direction, magnitude, and frequency (3, 27–29) alter trabecular bone structure during development, such that this structure provides a 'functional record' of age-related behavioral changes (19–23, 28, 30–32). Mechanical stimuli initiate several cellular processes in osteocytes including gene activation, growth factor production, and matrix synthesis (33, 34). One method through which bone is thought to sense and adapt to mechanical stimuli is the strain-driven motion of interstitial fluid through the canaliculi that form the network of connections between osteocytes (1, 33). This signals the osteocytes to initiate bone modeling or remodeling. When strains are normalized, a balanced state

Author contributions: J.P.P.S. designed research; J.P.P.S. performed research; J.P.P.S. analyzed data; A.D.G. aided in data collection; and J.P.P.S., A.D.G., T.M.R., and J.T.S. wrote the paper.

The authors declare no competing interest.

This article is a PNAS Direct Submission.

[1]To whom correspondence may be addressed. Email: jpps2@cam.ac.uk.

This article contains supporting information online at https://www.pnas.org/lookup/suppl/doi:10.1073/pnas.2208772119/-/DCSupplemental.

Published December 2, 2022.

is reached in which bone formation and removal are roughly equal (35). Computer models that simulate strain energy associated with locomotion accurately predict the distribution of trabecular structure throughout a bone and the primary orientation of trabeculae (3, 36). Trabecular bone is most resistant to compression, less so to tension, and weakest in shear strains (37, 38). Therefore, bone functional adaptation may be driven by shear strain even in cases where compressive strains are greater (37, 39). Previous research on the ontogeny of trabecular bone in humans (19–22, 40–44), great apes (32, 45), and other mammals (31, 46, 47) suggests a strong link between changes in loading conditions as gait develops and responses in trabecular structure. For paleontologists, this offers intriguing potential for reconstructing developmental variation in locomotor loading conditions from juvenile fossils.

Trabecular Bone Ontogeny

Bone growth occurs via the transformation of growth plate cartilage into bone through a series of cell and matrix changes (48, 49). The transformation from growth plate cartilage to trabecular bone is similar among mammals (48). This process sets up a basic trabecular structure which can later be modified through metabolic and mechanical factors (3). Trabecular bone is laid out orthogonal to the growth plate in a dense and anisotropic structure which is later refined into bone- and species-specific heterogeneous adult states. After initial ossification, the underloaded elements of the dense trabecular structure are removed and additional bone is added in strained areas, resulting in a mechanically adapted state. This model correctly predicts observations of bone loss at early stages of ontogeny and explains it as the result of the removal of redundant material (3, 7, 36, 50).

A Model Linking Brain and Bone Development. In this paper, we aim to demonstrate that there are strong links between neuromuscular maturation, life history, locomotor ontogeny, and trabecular bone structure. This implies that trabecular structure of fossil subadults is a proxy for the rate of neuromuscular maturation and life history of extinct species. Here we discuss the theoretical justification of our approach and condense it into a testable model. The kinetics and kinematics of locomotion are transformed from an immature state to increasingly adult-like patterns during ontogeny (51, 52). Ontogenetic changes in locomotor loading are generated by neural circuits that develop in parallel to increases in physical size and weight of a growing animal (53). Various studies have found slight positive allometry between trabecular bone volume fraction (BV/TV) and body mass (54–57), but purely ontogenetic allometry does not explain age-related variation in trabecular properties during development (19–21, 23, 31, 41, 46) leaving room for other factors like ontogenetic variation in locomotor kinetics and kinematics due to neuromuscular maturation. Across mammals (58) and birds (59), adult brain size strongly predicts time to locomotor onset after conception rather than after birth, indicating that locomotor development occurs as part of a highly conserved developmental process. During early locomotor development, infants are mainly focused on minimizing the risk of falling (60–62). When individuals increase in strength, stability improves and postural constraints are reduced (41, 63, 64). Throughout ontogeny, the body refines the most optimal neural networks (53, 65), resulting in a reduction in the variability of muscle activation and co-contraction and the emergence of the adult gait (61, 64–67). It has long been recognized that central nervous system maturation and ontogenetic allometry must interact to produce age-related variation in animal locomotion (52). In this paper, we merge this widely accepted understanding of locomotor development with 'bone functional adaptation,' a central paradigm in skeletal development (3, 68). Both theoretical paradigms are widely accepted in general forms although significant debates exist regarding their specific mechanistic underpinnings. We propose the following model to explain ontogenetic trajectories of trabecular bone structure (Fig. 1):

i. Trabecular structure is largely shaped by age-related variation in loading conditions.
ii. Changing gait kinetics during the development of locomotion alter a bone's mechanical environment to which trabecular structure dynamically adapts (3, 7, 20, 28).
iii. Changes in gait kinetics arise from interactions between maturation of the nervous system due to experience and brain development and increases in body mass due to somatic growth (52, 60, 65).
iv. Therefore, interactions between the degree of brain maturation and body mass should also predict age-related variation in trabecular structure.

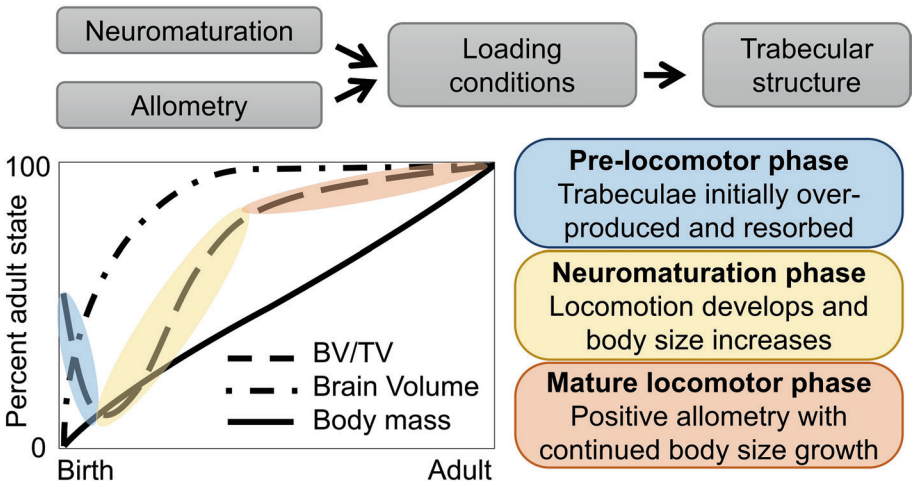

Fig. 1. Summary of our model describing age-related variation in BV/TV as an interaction between growth in body mass, neuromaturation, and locomotor mechanics. Adapted from Saers et al. (69).

Table 1. Summary of relevant life history variables: mean age of locomotor milestones and the mean age at eruption of the first and second molars (M1, M3)

Species	Locomotor onset	Locomotion adult-like	M1 eruption	M3 eruption[3]	Adult brain size approximated
Homo sapiens	1[1]	5–6[5,9]	6.3[3]	20.5	6*
Pan troglodytes	0.33[2]	4–6[2]	4.0[8]	11.2	4.5*
Gorilla gorilla	0.33[2]*	3–4[2]*	3.8[8]	10.9	3.4*
Macaca fuscata	0.08[4]	1.5[4]	1.6[3]	5.8	1.7[7]

All ages are species averages in years after birth.References: [1]Garwicz et al. (58)[2], Doran (25)[3], Smith et al. 75[4], Kimura 76[5], Sutherland (52), [6]Cofran and DeSilva 69, [7]Sakaiet al. 77, [8]Kelley and Schwartz 78, [9]Samson et al. 79.
*In the absence of published data on the timing of locomotor onset and adult-like locomotion in *G. gorilla*, data for these two variables are reported here for *G. beringei*.

The aim of this paper is to test this model based on analysis of a cross-sectional ontogenetic sample of the calcaneus of humans, chimpanzees, gorillas, Japanese macaques, and available biomechanical data from the published literature. These species cover several major primate locomotor modes including knuckle-walking/climbing (*Gorilla, Pan*), bipedalism (*Homo*), and terrestrial/arboreal quadrupedalism (*Macaca*). All species differ in life history, body size, sexual dimorphism, and locomotor ontogeny, enabling us to test support for our model despite such potentially confounding variables. There are several reasons why the calcaneus is an excellent bone for this study. The calcaneus is present at birth in all four species and is one of the last bones to complete ossification 70,71. In skeletal analysis, trabecular bone is modeled as a continuous material; however, this assumption breaks down on scales smaller than 3–5 trabecular lengths and along the edges of a bone 72. Fortunately, the calcaneus is relatively large and contains enough trabecular bone to satisfy the continuum assumption 72. The calcaneus has a highly species-specific loading environment as it contacts the ground in apes but serves solely as a lever in other primates. Applying our model to species where the calcaneus serves different functions can assess its general applicability.

The model predicts that interactions between body size and brain development underlie age-related variation in locomotor kinetics as organisms learn to walk, which should, in turn, result in age-related variation in trabecular bone structure. Marked changes in the slope with which trabecular structure varies with age are expected to correspond to landmark events in the development of locomotion like the onset of locomotion and the achievement of an adult-like gait. The ages at which locomotor and other developmental landmarks occur on average are summarized in Table 1. In each species, adult brain size develops well before adult body size is achieved 73. Additionally, in all but *Pan troglodytes* the males take longer than females to reach their adult body size 74. Locomotor development of humans, chimpanzees, gorillas, and Japanese macaques is described in *SI Appendix*, Supplementary information 1, and general calcaneus functional morphology is described in *SI Appendix*, Supplementary information 2.

Research Questions and Null Hypotheses. In this paper, we aim to demonstrate that there are strong links between locomotor loading, neuromuscular maturation, life history, and trabecular bone structure throughout ontogeny. We first assess whether average age-related changes in kinetic data in humans 79,80 chimpanzees 81, and Japanese macaques 76 can predict age-related variation in trabecular bone structure in age-matched individuals (Question 1). We then test the second part of the model by assessing whether interactions between neuromaturation and body mass can predict age-related patterns in kinetic data (Question 2). We then examine if this relationship between neuromaturation and allometry predicts ontogenetic trajectories of trabecular bone across primates (Question 3). Finally, we assess if landmark changes in the development of locomotion (locomotor onset, achievement of adult-like locomotor repertoire) are associated with distinct changes in the slope with which trabecular structure varies with age. If we can demonstrate that age-associated break points in BV/TV correspond to developments in locomotor kinetics and neuromaturation in extant primates, then researchers could similarly infer locomotor development and thus neuromaturation rates in fossil species.

1. Does age-related variation in locomotor loading predict BV/TV in humans, chimpanzees, and macaques?

We use kinetic data from the literature and age-match this to our measured trabecular bone properties in the calcaneus of humans, chimpanzees, and macaques. **H0:** Bone volume fraction (BV/TV) is not proportional to age-related variation in kinetic variables. We will reject the null hypothesis if there is a significant linear correlation between BV/TV and kinetic variables.

2. Do interactions between body mass and neuromaturation predict age-related variation in locomotor kinetics?

We then test whether interactions between age-related variation in brain development and body mass can predict age-related variation in hindfoot and ankle kinetics. **H0:** interactions between neuromaturation (or percentage of adult brain size) and body mass do not account for age-related variation in kinetic variables. We will reject the null hypothesis if there is a significant linear correlation between an interaction model between body mass and neuromaturation (or percent adult brain size) and kinetic variables and if the model quality is higher than any alternative (Lowest Akaike Information Criterion (AIC); 82).

3. Do interactions between body mass and neuromaturation predict ontogenetic trajectories of BV/TV in primates?

We compare various regression models to assess which best predicts age-related variation in trabecular bone properties. The model with the lowest AIC and highest R^2 is chosen as indicating the highest model quality. **H0:** interactions between percentage of adult brain size and body mass do not correlate with age-related variation in BV/TV in primates. We will reject the null hypothesis if interactions between body mass and percent of adult brain size are the highest quality models.

4. Do milestones in the development of locomotion correspond to significant changes in slope in the relationship between age and BV/TV?

Using piecewise linear regressions, we test if milestones in locomotor development match changes in slope of the relationship between age and BV/TV across four species. Locomotor landmarks are 1) onset of locomotion and 2) the achievement of adult-like locomotion. The model with the lowest AIC and highest R^2 is chosen as indicating the highest model quality. **H0:** break points in the slope of piecewise regressions do not overlap with the ages at which landmark changes in locomotion occur (Table 1). We reject the null hypothesis if piecewise regression models are higher-quality models compared to linear regressions and if the break points of piecewise regressions overlap with the ages of locomotor onset and the achievement of adult gait.

Table 2. Statistics summarizing the model outcomes of regressions between age-related variation in bone volume fraction (BV/TV) and kinetic variables

Species	Model	R^2	*P*	n
Homo	BV/TV ~ hindfoot FTI	0.93	<0.001	11
	BV/TV ~ whole foot FTI	0.93	<0.001	11
	BV/TV ~ peak ankle moment	0.83	<0.001	22
Pan	BV/TV ~ FTI	0.89	<0.001	36
	BV/TV ~ ankle moment (from mean GRF)	0.89	<0.001	36
	BV/TV ~ ankle moment (from FTI)	0.87	<0.001	36
Macaca	BV/TV ~ peak GRF resultant (2–6 mo old)	0.76	0.052	5
	BV/TV ~ peak GRF resultant (full sample)	0.79	<0.001	27
	BV/TV ~ peak ankle moment (2–6 mo old)	0.77	0.051	5
	BV/TV ~ peak ankle moment (full sample)	0.77	<0.001	27

FTI = force-time-integral normalized by body mass, GRF = ground reaction force.

Results

We first test whether age-related changes in BV/TV are associated with ontogenetic changes in locomotor kinetics (Question 1). We then investigate if age-related variation in locomotor kinetics (Question 2) and BV/TV (Question 3) is in turn associated with brain and body size growth in all species. Confirmation of these three questions implies that age-related variation in BV/TV is a proxy for both locomotor kinetics and neuromuscular maturation. Finally, we examine whether changes in the slope of age-related variation in bone volume fraction correspond to the age of the onset of locomotion and the age at which adult-like locomotion is achieved (Question 4).

Question 1. Does age-related variation in locomotor loading predict BV/TV in humans, chimpanzees, and macaques?

According to our model, BV/TV of the calcaneus should be predictable largely by age-related variation in its loading environment. We approximate loading environment using force-time-integrals (FTI), peak or mean ground reaction forces (GRF), and estimated peak or mean ankle joint moments. In humans, chimpanzees, and Japanese macaques, the biomechanical variables correlate strongly and linearly with BV/TV of the calcaneus (R^2= 0.76–0.93; Table 2 and Fig. 2). These results support the first part of our model that ontogenetic variation BV/TV can be predicted based on ontogenetic variation in the loading environment of the foot. We therefore reject null hypothesis 1.

Question 2. Do interactions between body mass and neuromaturation predict age-related variation in locomotor kinetics?

Our model predicts that the loading environment should vary depending on interactions between neuromuscular maturation and allometric scaling as body size increases. We tested whether age-related variation in locomotor kinetics of humans, chimpanzees, and macaques is best predicted by body mass, neuromaturation, or an interaction between body mass and neuromaturation. The neuromaturation variable is strongly and linearly correlated to percentage of adult brain size in humans (R^2= 0.98, $P < 0.001$). Since we have no way to estimate neuromaturation in the non-human primates, we use estimated percentage of adult brain size as a proxy. Almost all models are significant, but the highest quality models (highest R^2 and lowest AIC) are models that include interactions between neuromaturation (or percentage of adult brain size) and body mass (Table 3).

These strong model fits are consistent with an interaction between neuromaturation (and by proxy, percent adult brain size) and body mass underlying ontogenetic variation in locomotor kinetics observed in all three species, and we therefore reject null hypothesis 2. This strongly, but indirectly, supports our model that interactions between body mass and neural maturation explain age-related variation in loading patterns as gait develops.

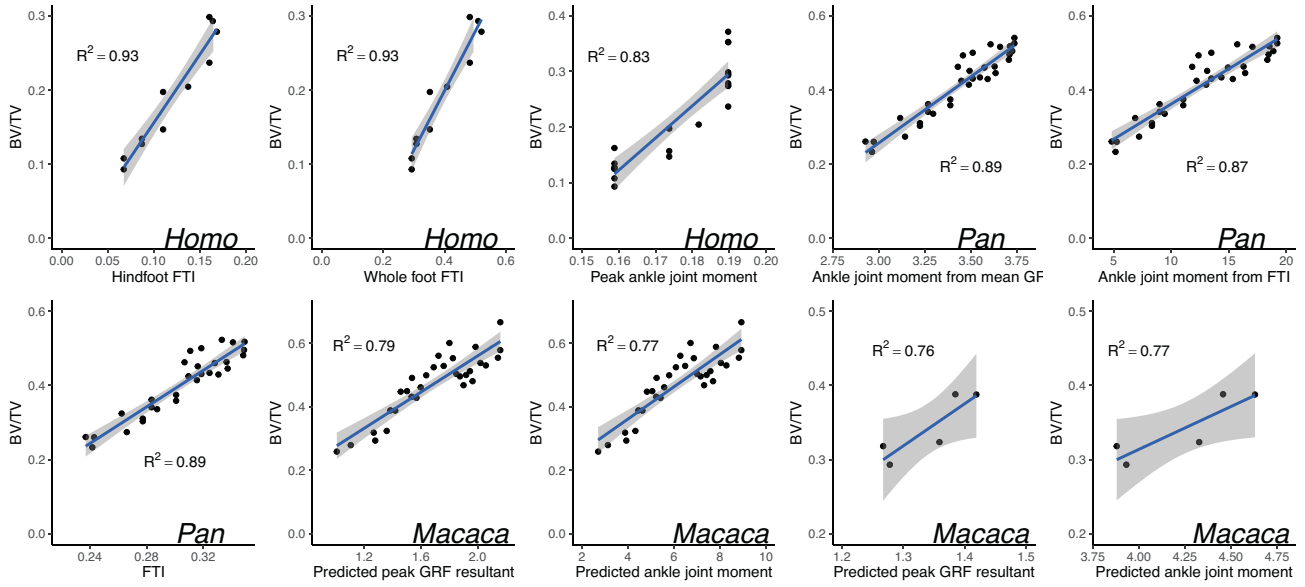

Fig. 2. Regressions between kinetic variables and calcaneal bone volume fraction (BV/TV) in ontogenetic samples of humans, chimpanzees, and Japanese macaques. Macaques are analyzed twice, first using a sample that matches the age range of the study from which kinetic variables were taken [2–6 mo, n = 5, 76]. Second, a larger sample using predicted kinetic variables for younger and older individuals keeping in mind that the equation used to predict these variables was derived from very young individuals and few datapoints. See *Materials and Methods* for further details. FTI = force-time-integral normalized by body mass, GRF = ground reaction force.

Table 3. Comparison of various regression models where age-related variations in loading conditions are predicted by body mass, neuromaturation, or an interaction between the two

Taxon	Dependent	Independent	Adj. R^2	AIC	*P*	n
Homo	FTI whole foot	BM	0.87	−43.50	<0.001	12
		Percent adult brain size	0.84	−40.64	<0.001	12
		Neuromaturation	0.98	−67.67	<0.001	12
		BM × neuromaturation	**0.99**	**−78.22**	**<0.001**	**12**
		BM × percent adult brain size	0.98	−64.55	<0.001	12
	FTI hindfoot	BM	0.77	−56.47	<0.001	12
		Percent adult brain size	0.94	−73.13	<0.001	12
		Neuromaturation	0.92	−69.59	<0.001	12
		BM × neuromaturation	0.98	−85.47	<0.001	12
		BM × percent adult brain size	**0.99**	**−93.25**	**<0.001**	**12**
	Peak ankle moment	BM	0.64	−142.81	<0.001	22
		Percent adult brain size	0.91	−173.27	<0.001	22
		Neuromaturation	0.73	−148.91	<0.001	22
		BM × neuromaturation	0.92	−176.44	<0.001	22
		BM × percent adult brain size	**0.95**	**−187.36**	**<0.001**	**22**
Pan	FTI	BM	0.84	−197.85	<0.001	35
		Percent adult brain size	0.84	−198.41	<0.001	35
		BM × percent adult brain size	**0.99**	**−285.02**	**<0.001**	**35**
	Ankle moment from mean GRF	BM	0.83	−59.28	<0.001	35
		Percent adult brain size	0.86	−66.61	<0.001	35
		BM × percent adult brain size	**0.99**	**−152.01**	**<0.001**	**35**
	Ankle moment from FTI	BM	0.91	122.12	<0.001	35
		Percent adult brain size	0.74	160.49	<0.001	35
		BM × percent adult brain size	**0.98**	**66.02**	**<0.001**	**35**
Macaca	Peak GRF 2–6 mo	BM	0.68	−13.66	0.087	5
		Percent adult brain size	1.00	−55.21	<0.001	5
		BM × percent adult brain size	**1.00**	**−111.74**	**<0.001**	**5**
	Peak ankle moment 2–6 mo	BM	0.68	2.20	0.085	5
		Percent adult brain size	1.00	−33.24	<0.001	5
		BM × percent adult brain size	**1.00**	**−73.50**	**<0.001**	**5**
	Peak GRF Full sample	BM	0.87	−43.63	<0.001	30
		Percent adult brain size	0.99	−133.93	<0.001	30
		BM × percent adult brain size	**1.00**	**−204.20**	**<0.001**	**30**
	Peak ankle moment Full sample	BM	0.91	50.04	<0.001	30
		Percent adult brain size	0.98	0.68	<0.001	30
		BM × percent adult brain size	**1.00**	**−69.32**	**<0.001**	**30**

Highest quality models in bold (lowest AIC, highest R^2).FTI = force-time-integral normalized by body mass, GRF =ground reaction force, BM = body mass.

Question 3. Do interactions between body mass and brain development predict ontogenetic trajectories of BV/TV in primates?

In all four species, the age-related variation in BV/TV is best predicted by an interaction between body mass and percentage of adult brain size (Table 4). However, in humans and macaques the best-fitting model also includes another interaction term for the age of locomotor onset (see Table 1). This is due to the reversal in slope that occurs around the onset of locomotion (Fig. 4). Presumably, a slope reversal at the onset of locomotion also occurs in chimpanzees and gorillas, but the youngest *Gorilla* and *Pan* specimens in our sample are both estimated to be around 6 mo of age, which is after the onset of independent locomotion around for both taxa (Table 1). These findings support the rejection of null hypothesis 3.

Predictions of the highest quality models are plotted in Fig. 3 against both chronological age and a measure of postnatal maturity (maturity = age / age at adulthood, birth = 0, adult = 1). In humans, the reversal from negative to positive slope is delayed compared to Japanese macaques in terms of chronological age and degree of postnatal maturity.

Question 4. Do milestones in the development of locomotion correspond to significant changes in slope in the relationship between age and BV/TV?

Using piecewise linear regressions, we examine whether models with zero, one, or two inflection points are better fits to the data (Table 5 and Fig. 4). In all four species, the piecewise models have the greatest model quality (highest R^2, lowest AIC). In humans and Japanese macaques, the highest quality model contains two break points: the first conforms to the age of locomotor onset (1 y in humans, 1 mo in macaques, Table 1), and the second conforms to the age where locomotor patterns match those of adults (around 5–6 y in humans and in the second year of life in Japanese macaques). In chimpanzees and gorillas, the best models

Table 4. Comparison of various regression models to predict BV/TV, the best fit (highest R^2) and highest model quality (lowest AIC) are in bold

Taxon	Independent variables	Adj. R^2	AIC	p
Homo sapiens (n = 26)	BM	0.69	−80.9	<0.001
	Percent adult brain size	0.28	−58.9	0.006
	BM × percent adult brain size	0.80	−92.1	<0.001
	BM × percent adult brain size × locomotor onset	**0.89**	**−105.3**	**<0.001**
Macaca fuscata (n = 35)	BM	0.67	−93.3	<0.001
	Percent adult brain size	0.58	−85.4	<0.001
	BM × percent adult brain size	0.73	−100.6	<0.001
	BM × percent adult brain size × locomotor onset	**0.85**	**−54.1**	**<0.001**
*Pan troglodytes (n = 32)**	BM	0.76	−103.6	<0.001
	Percent adult brain size	0.76	−102.8	<0.001
	BM × percent adult brain size	**0.81**	**−109.1**	**<0.001**
*Gorilla gorilla (n = 38)**	BM	0.68	−104.6	<0.001
	Percent adult brain size	0.72	−109.4	<0.001
	BM × percent adult brain size	**0.89**	**−145.2**	**<0.001**

BM = body mass in kg, *No individuals pre-locomotor onset in the sample.

Table 5. Comparison of linear regressions between BV/TV and age to piecewise regression models with one or two break points

Taxon	Number of breaks	Break points ± se	Adj. R^2	AIC
Homo sapiens (n = 26)	0		0.72	−83.4
	1	0.5 ± 0.1	0.87	−103.3
	2	**0.9 ± 0.1, 6.4 ± 1.6**	**0.91**	**−112.0**
Macaca fuscata (n = 36)	0		0.61	−90.4
	1	1.6 ± 3.1	0.79	−111.1
	2	**0.06 ± 0.07, 1.41 ± 0.17**	**0.86**	**−123.5**
Pan troglodytes (n = 32)	0		0.78	−106.7
	1	**4.9 ± 0.6**	**0.90**	**−131.8**
	2	4.9 ± 1.3, 6.7 ± 5.1	0.90	−129.1
Gorilla gorilla (n = 38)	0		0.77	−118.0
	1	**2.9 ± 0.7**	**0.86**	**−135.1**
	2	0.7 ± 0.1, 2.9 ± 1.0	0.86	−133.3

Break points correspond to the age in years where the bivariate relationship between age and BV/TV changes significantly in slope.0 breaks = standard linear regression, one break = piecewise regression with one inflection point, two breaks = piecewise regression with two inflection points.

only contained one break point. Presumably, the reason is that for both species, the youngest individuals are around 6 mo of age which is after the onset of locomotion. The single break points in chimpanzees and gorillas also occur at the age at which locomotor patterns become nearly identical to that of adults which is on average around 5 y for chimpanzees and around 3.5 y for gorillas. We therefore reject null hypothesis 4.

Discussion

All null hypotheses were rejected, and the results support the predictions of our model wherever data were available to test it (Fig. 1). We found that ontogenetic variation in kinetic data strongly and linearly predicts age-matched BV/TV in humans, chimpanzees, and Japanese macaques. We predicted that age-related variation in these biomechanical variables is the product of variation in gait kinetics due to neuromuscular maturation and somatic growth. Results were also consistent with this prediction as the interaction between body mass and a derived equation for neuromaturation and estimated percentage of adult brain size were also the best models fitted to ontogenetic variation in estimates of FTI, GRF, and ankle joint moment. These results strongly support the hypothesis that trabecular bone is shaped by age-related variation in loading environment during ontogeny which is in turn the product of neuromaturation and body size growth. Our results suggest that analysis of trabecular bone ontogeny may provide a novel approach for assessing the neural maturation of fossil vertebrates. We discuss how these findings can be applied to the fossil record below.

Our findings are consistent with the interpretation that the developmental trajectory of BV/TV from conception to adulthood is marked by three main phases that can be identified by significant changes in slope of the bivariate relationship between BV/TV and age (Fig. 1). The first 'pre-locomotor' phase occurs between the start of endochondral ossification until the onset of locomotion where bone is laid down orthogonal to the ossification center and subsequently resorbed, leading to a decrease in BV/TV 19,20,69. The second 'neuromaturation' phase occurs between the age at onset of locomotion and the achievement of adult-like gait and locomotor repertoire and is marked by a reorganization of trabecular structure into the heterogenous adult-like state and an increase in overall BV/TV (20, 23). Finally, the 'mature locomotion' phase starts around the beginning of the juvenile period when locomotor behavior becomes adult-like and ends with adulthood when growth has completed. When adult-like locomotion is achieved, humans are around 20% of adult body size, chimpanzees 25%, gorillas 15 to 30%, and Japanese macaques 25%. This final phase is marked by a shallow increase in BV/TV which corresponds to slight positive allometry between body mass and BV/TV which has been reported within and between primates (20, 23, 54, 55) and other animals 56,83.

Pan and *Gorilla* data analyzed here do not show the reduction in BV/TV after birth that is found in *Homo* and *Macaca*. This conforms to previous reports in the chimpanzee postcranium by Tsegai and colleagues (32) who also did not find an initial reduction in BV/TV. However, both studies lack individuals younger

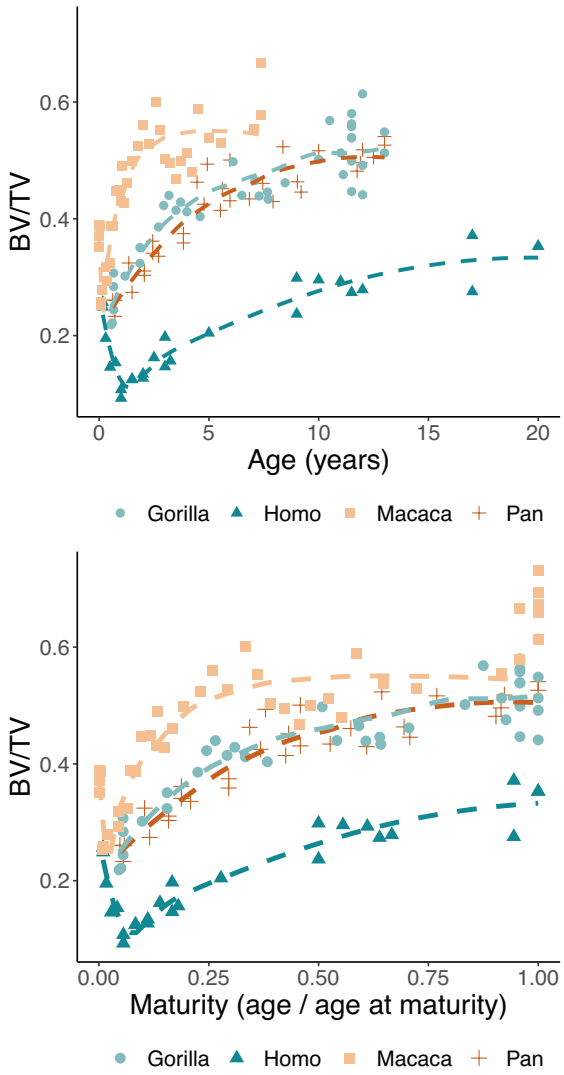

Fig. 3. Trabecular bone volume fraction plotted against chronological age (*Left*) and maturity score (age/age when growth ceases on average, adults have a value of 1; *Right*). Lines are loess curves fitted to predicted bone volume fraction (BV/TV) based on interactions between body mass and percent adult brain size (chimpanzees and gorillas) and interactions between body mass, percent adult brain size, and locomotor onset (humans and macaques).

than 6 mo. As the reversal in slope from negative to positive coincides with the onset of locomotion, which occurs well before 6 mo of age in *Gorilla* and *Pan*, a likely explanation for not observing the early reduction in BV/TV is a lack of neonates and very young infants in both samples (Fig. 4).

The onset of locomotion occurs relatively late in humans after birth due to their large adult brain size (58) and relatively short gestation 84–86. Portmann 87 estimated that if humans were to be born as neurologically and cognitively precocial as chimpanzees, they would require a gestation time of at least 18 mo. This late onset of locomotion in both chronological age and developmental age is reflected in trabecular structure when the slope of BV/TV with age switches from negative to positive (Figs. 3 and 4). This finding implies that ontogenetic trajectories of trabecular structure offer a unique opportunity to study variation in the relative timing of locomotor onset in the fossil record. Interestingly, for all four species in this study, the age at locomotor maturation overlaps roughly with the timing of the eruption of the first molar, the age at which the brain approximates the size of an adult, and the beginning of the juvenile phase of primate development (Tables 1 and 5). Such correspondence between life history-related variables is perhaps not surprising given the interconnected developmental mechanisms that give rise to the commonly shared life history stages of primates 73,86,88. In non-human primates, the transition from infancy to the juvenile period is roughly marked by independence of the subadult from its mother, advanced motor control, the eruption of the first permanent molars, sexual immaturity, and reduced growth velocity compared to infancy 86. Humans are the exception to the general primate developmental pattern due to the presence of a unique childhood phase between infancy and juvenility which is characterized by reduced growth velocity and weaning, but combined with continuing brain growth, immature dentition, and a dependence on older individuals for care and feeding 86,89,90. Our results support the idea that trabecular bone structure reflects the advanced motor control of primates at the start of the juvenile phase via its close correspondence to the adult-like state. Our results also support the prediction of our model of a 'mature locomotor phase' where minor differences in trabecular properties between juveniles and adults can be attributed to slight positive allometry with body size that has been reported within and between primate species (23, 54, 55).

Implications. The results support our proposed model to explain species-specific variation in the developmental trajectories of trabecular bone structure. Support for this model is particularly noteworthy as all four species differ in potentially confounding variables such as life history, body size, sexual dimorphism, and locomotor ontogeny. These results point to fundamental links between brain development and associated life history strategies, on the one hand, and locomotor development and trabecular bone structure on the other. Simple interactions between body mass and neuromaturation also predict BV/TV across the four primate species in our sample, implying that age-related variation in BV/TV can be used to infer the rate of neuromuscular maturation of locomotion, given an adequate sample size. This implies that trabecular structure can be used to reconstruct key life history events in fossil species including the onset of locomotion and the timing at which adult-like locomotor patterns are obtained.

In humans, the onset of locomotion is associated with the timing of several important aspects of brain development. Locomotion is not just a developmental precursor to numerous psychological changes but plays a causal role in their formation 91–94. The onset of human independent locomotion is followed by a revolution in perception-action coupling, spatial cognition, memory, and social and emotional development 91. Neural function and structure reciprocally influence one another throughout development 91,92, placing the activity of locomotor development in the center of development, rather than being just a consequence of neural maturation. In other words, the onset of independent locomotion is an important life history event related to adult brain size and the timing of neuromuscular development. Being able to detect bony markers of locomotor development can provide unique insights into fossil locomotion as well as aspects of life history 95.

Our findings show that simple bivariate plots of age and whole bone BV/TV are sufficient to reconstruct the timing of locomotor onset and maturation in fossil species. These data are easy to generate using the protocols and free software described in this manuscript. A drawback of this approach is that a sample consisting of multiple individuals is required to pinpoint inflection points in slope. Isolated fossils contain

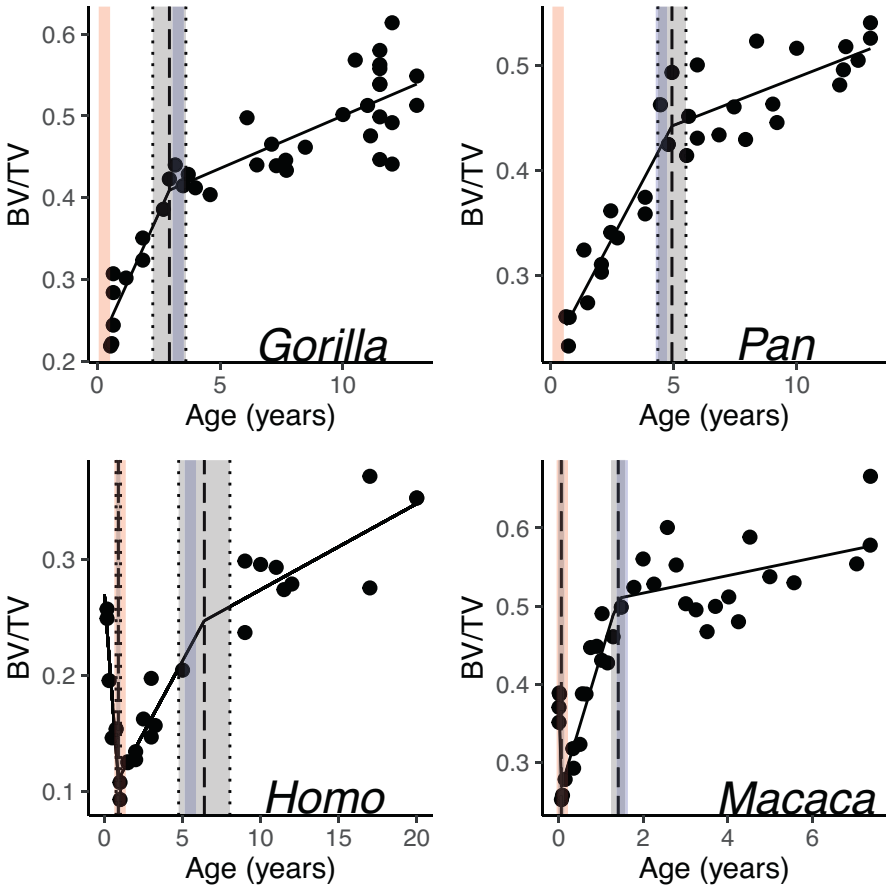

Fig. 4. Best-fitting piecewise regression models from Table 4. Gray-shaded areas represent the standard error of the break points, red-shaded areas represent mean age of locomotor onset, and blue-shaded areas represent mean age of locomotor maturation. BV/TV = bone volume/total volume.

additional morphological signatures of locomotor onset that have been presented previously (20, 23). Specifically, we showed that primary direction of trabecular bone stiffness reorients from the direction in which the bone is growing to the direction in which the bone is loaded (80°) exactly as locomotor onset occurs (23). Precise calculation of primary bone stiffness requires specialized software to which we no longer have access (Medtool, www.dr-pahr.at). However, assessment of whether the trabecular reorientation has occurred can be done visually, providing an indicator of locomotor onset that is applicable even to isolated fossils.

The fossil record provides several challenges to the application of our approach. Issues include those common to all paleobiology such as preservation, dating, dealing with isolated finds, taxonomy, as well as those specific to studies of development such as the estimation of chronological age and developmental stage. The chronological age of fossil specimens can be estimated based on developmental indicators such as body size, brain development, dental eruption, and skeletal fusion. Synchrotron scanning of the dentition can be used to establish a chronological age for an individual 96, at least within the first few years after birth. Such chronological ages can then be used to calibrate ontogenetic trajectories of somatic, dental, and brain development 97. Juvenile hominin fossils are exceptionally rare, but recent discoveries of numerous juvenile hominins 98 paired with methodological advances in the functional analysis of trabecular bone 23,99 provide a unique opportunity to investigate hominin locomotor ontogeny. More broadly, this approach can provide novel insights into the evolution and development of two defining human traits: our slow development and our unique mode of locomotion.

Limitations. The analyses reported here can be expanded by examining additional skeletal elements, inclusion of additional trabecular variables (trabecular thickness, anisotropy), and by mapping regional variation in trabecular properties throughout whole bones (23). Like most biomechanical analyses of trabecular bone structure, we use a cross-sectional approach, linking ontogenetic variation in average foot loading measured in one group, to age-related variation in trabecular bone structure measured in another. Our biomechanical data does not account for age-related variation in daily time spent walking or running, nor for inter-individual variation in walking mechanics. Longitudinal approaches are currently possible in rodents and are slowly becoming more feasible in humans and other large mammals with advances in HRpQCT scanning. The next step to investigate the relationships between bone structure, behavior, and neural development should take advantage of these exciting possibilities for longitudinal experiments. The use of inference and induction, based on existing cross-sectional analyses and data, provides an excellent first attempt at linking neural development, the motor control of locomotion, and trabecular bone morphology. We hope that this paper will inspire and encourage researchers in a range of fields to attempt the longitudinal studies that would be ideal to experimentally validate the models and results tested here.

Conclusions

In this paper, we placed the relationship between locomotor ontogeny and trabecular bone morphology into the broader developmental context of neural development, locomotor control, and ultimately life history. It has long been recognized that central nervous system maturation and ontogenetic allometry must interact to produce age-related variation in animal locomotion (52). We merge this widely accepted understanding of locomotor development with bone functional adaptation, a central paradigm in skeletal development (3, 68). We examined the ontogenetic trajectories of trabecular bone structure in the calcaneus of humans, chimpanzees, gorillas, and Japanese macaques. We showed that:

1. Ontogenetic variation in locomotor kinetics is strongly and linearly correlated with age-matched BV/TV in humans, chimpanzees, gorillas, and Japanese macaques.
2. Interactions between body size and percent adult brain size strongly predict ontogenetic trends in these biomechanical variables.
3. This interaction between percent adult brain size and body mass is the best model to explain age-related variation in BV/TV in all four primate species.
4. Distinct changes in the slope of the bivariate relationship between age and BV/TV correspond to the age of the onset of locomotion and the age at which adult-like locomotion is achieved.

Our results support the presence of fundamental links between brain development and associated life history strategies, on the one hand, and locomotor development and trabecular bone structure on the other. We therefore argue that ontogenetic variation in trabecular structure contains novel information regarding the rate of neuromuscular maturation and major life history events in fossil taxa. We discussed the implications of these results and how they can be applied to the fossil record. Further development of this approach could have significant implications for vertebrate paleontology by providing a new way of assessing the neural maturation of fossil vertebrates and would provide a new way in which paleobiologists can view the developing skeleton.

Materials and Methods

Sample. We micro-CT (μCT) scanned the calcaneus from the skeletal remains of 36 juvenile male Japanese macaques (*Macaca fuscata fuscata*) from a colony housed in a large open-air enclosure at the Primate Research Institute, University of Kyoto (PRI) 100. Individuals are of known age and body mass at death, and in most cases, parental lineage is recorded. Specimens were CT scanned at the PRI with a SkyScan1275 μCT scanner at 95 kV and 95 μA for 2,400 projections with an exposure of 0.216 s. CT scans were saved as 16 bit tiff stacks with isotropic voxel dimensions between 16 and 22 μm depending on bone size.

The gorilla (*Gorilla gorilla*, n = 38) and chimpanzee (*Pan troglodytes*, n = 32) specimens derive from the Powell Cotton Museum, Kent, UK. Age was estimated using dental eruption 101 and tooth formation stages using CT scans of the mandible 102. Body mass predicted from femoral head diameter following ontogenetic regression equations by Burgess et al. 75 [BM_{Pan}=exp(ln(FHD) × 2.88–6.27); $BM_{Gorilla}$=exp(ln(FHD) × 3.08–7.14)].

The human calcanei used in this study are derived from two archeological contexts and have both been published previously (see ref. 20 for further details, n = 26). Age was estimated by dental eruption and skeletal epiphyseal fusion using fusion times 78,103. Body mass in kilograms was estimated using age-specific femoral head diameter equations 104.

The human, gorilla, and chimpanzee specimens were scanned using an identical protocol with a Nikon XTH 225 ST HRCT laboratory scanning system at the University of Cambridge using energy settings optimized for the contrast between bone and air (125 kV, 135 μA, 1,080 views, 1,000ms exposure).

Calculating Neuromaturation of Human Locomotion. An equation to estimate neuromaturation of human locomotion was derived by Vaughan and colleagues (63). They show that non-dimensional scaling of velocity accounts for physical growth, yielding insight into the process of neuromaturation independent of size. Neuromaturation of locomotion for age was calculated using the equation $\beta = 0.45 \times (1\text{-}e^{-0.05*t})$, where t = age in months and β is a dimensionless value for neuromaturation of locomotion. As the neuromaturation equation was only derived for humans and would be unavailable in fossil taxa, we use percentage of average adult brain size as a proxy for neuromaturation as detailed below. Although the brain continues to develop after reaching its adult size, the experimentally derived measurement of neuromaturation is strongly linearly correlated with our estimate of percentage of adult brain size (R^2= 0.98, $P <$ 0.001) despite both measurements were derived by completely different studies, authors, and datasets.

Estimating Percentage Adult Brain Size. Percentage brain volume for age in Japanese macaques was estimated by combining data from two studies 105,106 and dividing by the average adult brain volume for a Japanese macaque 77,106 105.6 cm^3. We then used the following equation to predict percent adult brain size (PB) in macaques:

$$PB_{Macaca} = 0.7417 \times age^{0.0681}$$

We used data from Cofran and Desilva (107) to calculate equations to estimate percentage of adult brain size for age in chimpanzees, gorillas, and humans. We used Q-Q plots to show that brain size development was best modeled using a logarithmic function in humans and a power equation in gorillas. However, neither of these were a good fit to the chimpanzee data. Instead, we used a composite equation where brain size was estimated using different equation in three age groups. The following equations fit the data best:

$PB_{Homo} = (212.94 \times \ln(age) + 859.1)/1{,}260$

PB_{Pan}:

*0.5–2 y: $-0.0504 \times age^2 + 0.322 \times age + 0.3876$.

*2–4 y: $-0.015 \times age^2 + 0.145 \times age + 0.6$.

*4–15 y: $0.0454 \times \ln(age) + 0.8771$.

$PB_{Gorilla} = 0.8355 \times age^{0.1462}$

Calculation of Trabecular Bone Properties. TIFF stacks derived from μCT were segmented into bone and non-bone using the maximum entropy method in ImageJ (108) and then imported into ORS Dragonfly [Object Research Systems (ORS) Inc, Montreal, CA (109)]. Next, the cortical shell was isolated and removed from the internal marrow cavity using the Kohler segmentation algorithm (110). This step involved manually adjusting a slider until the cortical shell was entirely selected. After these segmentation steps, ORS Dragonfly was used to automatically calculate average bone volume fraction (bone volume/total volume, BV/TV) in the whole calcaneus.

Estimating Ontogenetic Variation in Calcaneus Loading Across Species. Trabecular bone structure is thought to adapt in ways that reduce strain in a bone caused by mechanical loading (3, 111–113). Strain energy is defined as the energy stored in a body due to deformation. Finite element analysis of the human calcaneus throughout stance during walking and running has shown that total strain energy is by far the greatest during push-off phase around 60 to 70% of stance (113). This total strain energy is the result of compressive joint reaction forces and tensile muscle forces which create a moment about the ankle joint (114). The joint reaction forces, moments, and total strain energy in the human calcaneus all reach their respective peak values during the toe off phase of stance (113). Analysis of this finite element data shows that total calcaneus strain energy is perfectly linearly correlated by the moment about the ankle joint during the propulsive phase of stance. There is a strong linear correlation between ankle joint moment and total strain energy (R^2= 1.0) as well as joint reaction forces and the tensile force exerted by the Achilles tendon (R^2= 0.97–0.99, *SI Appendix*, Supplementary information 3).

Terrestrial quadrupedal locomotion in primates is 'hindlimb-driven' with significantly greater peak propulsive and vertical GRF being generated by the hindlimbs compared to the forelimbs (115). Like humans, peak ankle joint moments

in terrestrial quadrupedal locomotion in chimpanzees 81,116 and macaques 76 occur during the propulsive phase. Based on the data summarized in *SI Appendix*, Fig. S1, the greatest strain energy in the calcaneus would be expected to occur during 'push-off' when the hip, leg, and ankle extensors push off from the ground to propel the individual forward. Since trabecular bone density generally corresponds to peak strain energy (3, 113), and the greatest strain energy density occurs at push-off when the calcaneus does not contact the ground, we expect that ontogenetic variation in trabecular bone density should correlate with age-related variation in peak ankle joint moment in species that use a heel strike gait (African apes) and those that do not (macaques).

Calculation of Ontogenetic Variation in Locomotor Kinetics Per Species. Data reflecting ontogenetic variation in locomotor kinetics were taken from the literature. The highest quality data were found for humans, some kinetic data were available for chimpanzees and Japanese macaques, but no kinetic data were available for gorillas. Three variables were used:

- GRF: The force exerted by the ground on a body in contact with it normalized by body mass. The greatest GRFs occur in the vertical direction, but substantial forces can also be generated in the sagittal and coronal planes. The combination of all GRFs is the resultant force. All units in percentage of body mass (kg).
- FTI: The area underneath a force-over-time curve, which is equivalent to loading during a single step rather than peak load. Units in percentage of body mass (kg) × stance time (seconds).
- Ankle joint moment: A measure of the force that can cause an object to rotate about an axis (%BW*moment arm length). We demonstrated above that peak ankle joint moment directly correlates with peak calcaneus strain energy during a step. Peak joint moment is a better proxy for age-related variation in ankle joint loading than GRFs as it incorporates age-related variation in moment arms and the kinematics of limb segment angles during propulsion. However, these variables are less straightforward to measure than GRFs and require kinetic and kinematic data to estimate (117). Units in percentage of body mass × moment arm length.

Humans. Dynamic foot loading data from 7,788 German children aged 1–13 y of age were taken from an experimental study 80. Participants were assessed by walking at self-selected speeds. FTI for the whole foot and hindfoot from 80 were age-matched to our historical sample (11 individuals aged between 1 and 13). We collected peak ankle joint moments from a different study on growing children aged between 1 and 7 y of age 79. The ankle joint moments showed adult-like patterns in 5-y-old children onwards; therefore, these data were used to estimate peak ankle joint moment for our whole skeletal sample aged over 1 y of age when locomotor onset occurs (n = 22).

Chimpanzees. Kimura 81 reported mean vertical, braking, and propulsive GRF components for subadult chimpanzees aged 1, 2, 3, 7, and 19 y old. FTI was calculated by multiplying mean GRF resultant by cycle duration. The relationship between age and FTI in this sample follows a linear exponential equation ($FTI_{resultant} = 0.2523*age^{0.1307}$, $R^2 = 0.71$, $P < 0.05$). We used this function to predict the FTI from age in our sample of chimpanzee calcanei. In addition, we also calculated the vertical moment generated about the ankle joint by the Achilles tendon using the following static calculation on the same dataset:

$M = F*R$,

where M is the ankle joint moment, F is the vertical GRF (in %BW) or FTI (in %BW*cycle duration), and R is the moment arm. Foot lever length (R) was estimated from Fig. 2 in ref. 81 which illustrates typical walking postures for age. R was taken as the distance from the ankle joint to the tarsometatarsal joint. There are a few reasons to be cautious with this calculation. First, it uses the mean vertical GRF and FTI, while our human data use peak GRF. Second, during an actual step the moment arm (R) would change depending on the angle of the ankle and the location of the center of pressure. This essentially estimates a scenario where the mean GRF or FTI during a step is applied statically with the foot flat on the ground and a center of pressure just under the first metatarsal head. Therefore, these estimations do not directly correspond to peak ankle moments that are used for humans. The estimated ankle joint moments correlate strongly with age and are best predicted using exponential functions:

Ankle joint moment predicted from mean GRF = $3.0421*age^{0.0801}$, $R^2 = 0.87$, $P < 0.03$).

Ankle joint moment predicted from FTI = $6.003*age^{0.4536}$, $R^2 = 0.99$, $P < 0.003$).

Using these equations, we predicted ankle joint moments based on age for our sample of chimpanzee calcanei, keeping in mind the caveats discussed above.

Japanese macaques. Kimura 76 reports age-related variation in peak GRF components and cycle duration in Japanese macaques. The sample includes three datapoints in the first 6 mo of age and then one point representing adults. The adults are quite old (2/3 in their 20 s) and may therefore not represent the average adult and the absence of datapoints in between means that patterns in the data will be highly sensitive to variation between individuals. As such it was not possible to fit a reliable equation to this dataset when including the adults. However, the data covering the first 6 mo of age are suitable and cover the period of most rapid locomotor development. We estimated peak ankle moment by multiplying peak GRF resultant by an estimation of lever arm length (0.5*estimated foot length). We then fit the following equations to the relationships between age and peak resultant GRF and peak ankle joint moment:

Peak resultant GRF = $0.3131*\ln(age) + 2.292$; $R^2 = 0.986$.

Peak ankle joint moment = $1.8538*\ln(age) + 5.0443$, $R^2 = 1$.

We used these equations to predict age-related variation in peak GRF and ankle moment in our sample of individuals aged between 2 and 6 mo of age (n = 5). We also used these equations to predict these variables for younger and older individuals keeping in mind that the equation was derived from very young individuals and few datapoints.

Statistical Analysis. Linear regressions and interactions between trabecular properties, age, brain maturation, and body mass were performed in R version 4.0.2 using the lm() function 82. When comparing various regression models, the model with the lowest Akaike Information Criterion (AIC (118)) and highest R^2 was chosen as indicating the highest model quality. Adding additional variables to a regression always increases the fit (R^2) due to spurious correlations. This process is called overfitting and causes the model to learn too much from the data, resulting in poor predictive power for non-measured samples. AIC measures the degree to which a model is overfit with lower values indicating a greater model quality (118, 119). We ran piecewise regressions using the 'segmented' R package (120) to investigate the presence of significant changes in slope of the relationship between age and trabecular structure. Piecewise regression is a useful technique for finding significant changes in slope in the relation between a dependent and independent variable. The technique uses dummy variables and an interaction term to split a linear regression into multiple segments. The least squares method is applied separately to each segment, by which the two regression lines are made to fit the dataset as closely as possible while minimizing the sum of squares of the differences between observed and predicted values of the dependent variable. We compared models with two, one, or no break points and chose the model with the lowest AIC as the highest quality model. Alpha level was set to 0.05 for all statistical tests.

Data, Materials, and Software Availability. All study data are included in the article and/or *SI Appendix*.

ACKNOWLEDGMENTS. We are grateful to Dr. Takeshi Nishimura (Primate Research Institute, Inuyama, Japan) and Dr. Rachel Jennings (Powell Cotton Museum, UK) for providing access to the primate sample. Funding: RCUK/BBSRC BB/R01292X/1, travel to the PRI was facilitated by a grant from the DM McDonald Fund, University of Cambridge.

Author affiliations: [a]Naturalis Biodiversity Center, 2333 CR Leiden, the Netherlands; [b]Department of Anthropology, University at Albany, SUNY, Albany, NY 12222; [c]Department of Anthropology, Pennsylvania State University, University Park, State College, PA 16802; and [d]Department of Anthropology, Western University, London, CA ON N6A 5C2

1. J. D. Currey, *Bones: Structure and Mechanics* (Princeton University Press, 2002).
2. R. Huiskes, R. Ruimerman, G. H. van Lenthe, J. D. Janssen, Effects of mechanical forces on maintenance and adaptation of form in trabecular bone. *Nature* **405**, 704–706 (2000).
3. D. R. Carter, G. S. Beaupré, *Skeletal Function and Form: Mechanobiology of Skeletal Development, Aging and Regeneration* (Cambridge University Press, 2001).
4. B. Hallgrímsson, K. Willmore, B. K. Hall, Canalization, developmental stability, and morphological integration in primate limbs. *Am. J. Phys. Anthropol.* **45**, 131–158 (2002).
5. M. L. Zelditch, F. L. Bookstein, B. L. Lundrigan, The ontogenetic complexity of developmental constraints. *J. Evol. Biol.* **6**, 621–641 (1993).
6. J. P. P. Saers, Y. Cazorla-Bak, C. N. Shaw, J. T. Stock, T. M. Ryan, Trabecular bone structural variation throughout the human lower limb. *J. Hum. Evol.* **97**, 97–108 (2016).
7. D. R. Carter, M. C. H. Van Der Meulen, G. S. Beaupré, Mechanical factors in bone growth and development. *Bone* **18**, S5–S10 (1996).
8. T. L. Kivell, A review of trabecular bone functional adaptation: What have we learned from trabecular analyses in extant hominoids and what can we apply to fossils? *J. Anat.* **228**, 569–594 (2016).
9. M. M. Skinner *et al.*, Human-like hand use in Australopithecus africanus. *Science* **347**, 395–400 (2015).
10. N. B. Stephens *et al.*, Trabecular architecture in the thumb of Pan and Homo: Implications for investigating hand use, loading, and hand preference in the fossil record. *Am. J. Phys. Anthropol.* **161**, 1–17 (2016).
11. T. M. Ryan *et al.*, Human-like hip joint loading in Australopithecus africanus and Paranthropus robustus. *J. Hum. Evol.* **2018**, 1–13 (2018).
12. A. Zeininger, B. A. Patel, B. Zipfel, K. J. Carlson, Trabecular architecture in the StW 352 fossil hominin calcaneus. *J. Hum. Evol.* **97**, 145–158 (2016).
13. P. J. Bishop *et al.*, Cancellous bone and theropod dinosaur locomotion. Part I–an examination of cancellous bone architecture in the hindlimb bones of theropods. *PeerJ* **6**, e5778 (2018).
14. A. Bardo *et al.*, The implications of thumb movements for Neanderthal and modern human manipulation. *Sci. Rep.* **10**, 1–12 (2020).
15. C. J. Dunmore *et al.*, The position of Australopithecus sediba within fossil hominin hand use diversity. *Nat. Ecol. Evol.* **4**, 911–918 (2020).
16. B. Hallgrímsson, B. K. Hall, *Variation* (Elsevier Academic Press, 2005), 10.1016/B978-0-12-088777-4.X5000-5.
17. S. J. Gould, *Ontogeny and Phylogeny* (Harvard University Press, 1977).
18. K. Kardong, *Vertebrates: Comparative Anatomy, Function, Evolution* (McGraw Hill Education, ed. 8, 2018).
19. T. M. Ryan, D. A. Raichlen, J. H. Gosman, "Structural and mechanical changes in trabecular bone during early development in the human femur and humerus" in *Building Bones: Bone Formation and Development in Anthropology*, C. J. Percival, J. T. Richtsmeier, Eds. (Cambridge University Press, 2017), pp. 281–302.
20. J. P. P. Saers, T. M. Ryan, J. T. Stock, Baby steps towards linking calcaneal trabecular bone ontogeny and the development of bipedal human gait. *J. Anat.* **236**, 474–492 (2020).
21. J. H. Gosman, R. A. Ketcham, Patterns in ontogeny of human trabecular bone from SunWatch Village in the Prehistoric Ohio Valley: General features of microarchitectural change. *Am. J. Phys. Anthropol.* **138**, 318–32 (2009).
22. T. M. Ryan, G. E. Krovitz, Trabecular bone ontogeny in the human proximal femur. *J. Hum. Evol.* **51**, 591–602 (2006).
23. J. P. P. Saers, A. D. Gordon, T. M. Ryan, J. T. Stock, Growth and development of trabecular structure in the calcaneus of Japanese macaques (Macaca fuscata) reflects locomotor behavior, life history, and neuromuscular development. *J. Anat.* **241**, 67–81 (2022).
24. L. A. Sarringhaus, L. M. MacLatchy, J. C. Mitani, Locomotor and postural development of wild chimpanzees. *J. Hum. Evol.* **66**, 29–38 (2014).
25. D. M. Doran, Ontogeny of locomotion in mountain gorillas and chimpanzees. *J. Hum. Evol.* **32**, 323–344 (1997).
26. F. Lacquaniti, Y. P. Ivanenko, M. Zago, Development of human locomotion. *Curr. Opin. Neurobiol.* **22**, 822–828 (2012).
27. C. Rubin *et al.*, Quantity and quality of trabecular bone in the femur are enhanced by a strongly anabolic, noninvasive mechanical intervention. *J. Bone Miner. Res.* **17**, 349–357 (2002).
28. M. M. Barak, D. Lieberman, J. Hublin, A Wolff in sheep's clothing: Trabecular bone adaptation in response to changes in joint loading orientation. *Bone* **49**, 1141–1151 (2011).
29. T. Sugiyama, J. S. Price, L. E. Lanyon, Functional adaptation to mechanical loading in both cortical and cancellous bone is controlled locally and is confined to the loaded bones. *Bone* **46**, 314–321 (2010).
30. H. Pontzer *et al.*, Trabecular bone in the bird knee responds with high sensitivity to changes in load orientation. *J. Exp. Biol.* **209**, 57–65 (2006).
31. C. F. Wolschrijn, W. A. Weijs, Development of the trabecular structure within the ulnar medial coronoid process of young dogs. *Anat. Rec.* **278**, 514–519 (2004).
32. Z. J. Tsegai, M. M. Skinner, D. H. Pahr, J.-J. Hublin, T. L. Kivell, Ontogeny and variability of trabecular bone in the chimpanzee humerus, femur and tibia. *Am. J. Phys. Anthropol.* **167**, 713–736 (2018).
33. E. H. Burger, J. Klein-Nulend, Mechanotransduction in bone: Role of the lacuno-canalicular network. *FASEB J.* **13**, 101–112 (1999).
34. S. Stewart, A. Darwood, S. Masouros, C. Higgins, A. Ramasamy, Mechanotransduction in osteogenesis. *Bone Joint Res.* **9**, 1–14 (2020).
35. P. Christen *et al.*, Bone remodelling in humans is load-driven but not lazy. *Nat. Commun.* **5**, 4855 (2014).
36. D. R. Carter, M. Wong, T. E. Orr, Musculoskeletal ontogeny, phylogeny, and functional adaptation. *J. Biomech.* **24**, 3–16 (1991).
37. J. G. Skedros, S. L. Baucom, Mathematical analysis of trabecular "trajectories" in apparent trajectorial structures: The unfortunate historical emphasis on the human proximal femur. *J. Theor. Biol.* **244**, 15–45 (2007).
38. T. M. Keaveny, E. F. Morgan, G. L. Niebur, O. C. Yeh, Biomechanics of trabecular bone. *Annu. Rev. Biomed. Eng.* **3**, 307–333 (2001).
39. Z. Wood *et al.*, Are we crying Wolff? 3D printed replicas of trabecular bone structure demonstrate higher stiffness and strength during off-axis loading. *Bone* **127**, 635–645 (2019).
40. A. Colombo *et al.*, Trabecular analysis of the distal radial metaphysis during the acquisition of crawling and bipedal walking in childhood: A preliminary study. *Bull. Mem. Soc. Anthropol. Paris* **31**, 43–51 (2019).
41. D. A. Raichlen *et al.*, An ontogenetic framework linking locomotion and trabecular bone architecture with applications for reconstructing hominin life history. *J. Hum. Evol.* **81**, 1–12 (2015).
42. F. Acquaah, K. A. Robson Brown, F. Ahmed, N. Jeffery, R. L. Abel, Early trabecular development in human vertebrae: Overproduction, constructive regression, and refinement. *Front Endocrinol. (Lausanne)* **6**, 1–9 (2015).
43. D. Reissis, R. L. Abel, Development of fetal trabecular micro-architecture in the humerus and femur. *J. Anat.* **220**, 496–503 (2012).
44. C. A. Cunningham, S. M. Black, Anticipating bipedalism: Trabecular organization in the newborn ilium. *J. Anat.* **214**, 817–829 (2009).
45. A. J. Ragni, Trabecular architecture of the capitate and third metacarpal through ontogeny in chimpanzees (Pan troglodytes) and gorillas (Gorilla gorilla). *J. Hum. Evol.* **138**, 102702 (2020).
46. B. M. C. Gorissen, C. F. Wolschrijn, A. A. M. van Vilsteren, B. van Rietbergen, P. R. van Weeren, Trabecular bone of precocials at birth; Are they prepared to run for the wolf(f)? *J. Morphol.* **277**, 948–956 (2016).
47. E. Tanck, J. Homminga, G. H. van Lenthe, R. Huiskes, Increase in bone volume fraction precedes architectural adaptation in growing bone. *Bone* **28**, 650–654 (2001).
48. S. Byers, A. Moore, R. Byard, N. Fazzalari, Quantitative histomorphometric analysis of the human growth plate from birth to adolescence. *Bone* **27**, 495–501 (2000).
49. A. M. Parfitt, R. Travers, F. Rauch, F. H. Glorieux, Structural and cellular changes during bone growth in healthy children. *Bone* **27**, 487–494 (2000).
50. P. Pivonka, A. Park, M. R. Forwood, *Functional Adaptation of Bone: The Mechanostat and Beyond*, P. Pivonka, Ed. (Springer, 2018).
51. J. W. Young, L. J. Shapiro, Developments in development: What have we learned from primate locomotor ontogeny? *Am. J. Phys. Anthropol.* **165**, 37–71 (2018).
52. D. Sutherland, The development of mature gait. *Gait Posture* **6**, 163–170 (1997).
53. H. Forssberg, Neural control of human motor development. *Curr. Opin. Neurobiol.* **9**, 676–682 (1999).
54. J. P. P. Saers, T. M. Ryan, J. T. Stock, Trabecular bone structure scales allometrically in the foot of four human groups. *J. Hum. Evol.* **135**, 102654 (2019).
55. T. M. Ryan, C. N. Shaw, Trabecular bone microstructure scales allometrically in the primate humerus and femur. *Proc. Biol. Sci.* **280**, 1–9 (2013).
56. M. Doube, M. M. Klosowski, A. M. Wiktorowicz-Conroy, J. R. Hutchinson, S. J. Shefelbine, Trabecular bone scales allometrically in mammals and birds. *Proc. Biol. Sci.* **278**, 3067–3073 (2011).
57. S. M. Swartz, A. Parker, C. Huo, Theoretical and empirical scaling patterns and topological homology in bone trabeculae. *J. Exp. Biol.* **201**, 573–590 (1998).
58. M. Garwicz, M. Christensson, E. Psouni, A unifying model for timing of walking onset in humans and other mammals. *Proc. Natl. Acad. Sci. U.S.A.* **108**, 433 (2009).
59. A. N. Iwaniuk, J. E. Nelson, Developmental differences are correlated with relative brain size in birds: A comparative analysis. *Can. J. Zool.* **81**, 1913–1928 (2003).
60. H. Forssberg, Ontogeny of human locomotor control I. Infant stepping, supported locomotion and transition to independent locomotion. *Exp. Brain Res.* **57**, 480–493 (1985).
61. J. A. Vilensky, E. Gankiewicz, Early development of locomotor behavior in vervet monkeys. *Am. J. Primatol.* **17**, 11–25 (1989).
62. J. A. Vilensky, Locomotor behavior and control in human and non-human primates: Comparisons with cats and dogs. *Neurosci. Biobehav. Rev.* **11**, 263–274 (1987).
63. C. L. Vaughan, N. G. Langerak, M. J. OMalley, Neuromaturation of human locomotion revealed by non-dimensional scaling. *Exp. Brain Res.* **153**, 123–127 (2003).
64. J. R. Hurov, Rethinking primate locomotion: What can we learn from development? *J. Mot. Behav.* **23**, 211–218 (1991).
65. N. Dominici *et al.*, Locomotor primitives in newborn babies and their development. *Science* **334**, 997–999 (2011).
66. T. Okamoto, K. Okamoto, P. D. Andrew, Electromyographic developmental changes in one individual from newborn stepping to mature walking. *Gait Posture* **17**, 18–27 (2003).
67. Y. Nakano, Footfall patterns in the early development of the quadrupedal walking of Japanese macaques. *Folia Primatol.* **66**, 113–125 (1996).
68. C. B. Ruff, "Biomechanical analyses of archaeological human skeletons" in *Biological Anthropology of the Human Skeleton*, A. M. Grauer, A. L. Katzenberg, Eds. (2018), pp. 189–224.
69. J. P. P. Saers, A. D. Gordon, T. M. Ryan, J. T. Stock, Growth and development of trabecular structure in the calcaneus of Japanese macaques (Macaca fuscata) reflects locomotor behavior, life history, and neuromuscular development. *J. Anat.* **241**, 1–15 (2022).
70. C. Cunningham, L. Scheuer, S. Black, *Developmental Juvenile Osteology* (ed. 2, 2016).
71. T. D. Smith, V. B. DeLeon, C. J. Vinyard, J. W. Young, *Skeletal Anatomy of the Newborn Primate* (Cambridge University Press, 2020), 10.1017/9781316591383.
72. T. Harrigan, M. Jasty, R. Mann, W. Harris, Limitations of the continuum assumption in cancellous bone. *J. Biomech.* **21**, 269–275 (1988).
73. S. R. Leigh, Brain growth, life history, and cognition in primate and human evolution. *Am. J. Primatol.* **62**, 139–164 (2004).
74. S. R. Leigh, Patterns of variation in the ontogeny of primate body size dimorphism. *J. Hum. Evol.* **23**, 27–50 (1992).
75. M. L. Burgess, S. C. McFarlin, A. Mudakikwa, M. R. Cranfield, C. B. Ruff, Body mass estimation in hominoids: Age and locomotor effects. *J. Hum. Evol.* **115**, 36–46 (2018).
76. T. Kimura, Development of quadrupedal locomotion on level surfaces in Japanese macaques. *Folia Primatol.* **71**, 323–333 (2000).
77. T. Sakai *et al.*, Developmental patterns of chimpanzee cerebral tissues provide important clues for understanding the remarkable enlargement of the human brain. *Proc. Biol. Sci.* **280**, 20122398 (2013).
78. J. Kelley, G. T. Schwartz, Dental development and life history in living African and Asian apes. *Proc. Natl. Acad. Sci. U.S.A.* **107**, 1035–1040 (2010).
79. W. Samson *et al.*, Foot mechanics during the first six years of independent walking. *J. Biomech.* **44**, 1321–1327 (2011).
80. S. Müller, A. Carlsohn, J. Müller, H. Baur, F. Mayer, Static and dynamic foot characteristics in children aged 1–13 years: A cross-sectional study. *Gait Posture* **35**, 389–394 (2012).

81. T. Kimura, Development of chimpanzee locomotion on level surfaces. *Hum. Evol.* **2**, 107–119 (1987).
82. R Core Team, *R: A Language and Environment for Statistical Computing* (R Foundation for Statistical Computing, Vienna, Austria, 2019).
83. M. Mielke *et al.*, Trabecular architecture in the sciuromorph femoral head: Allometry and functional adaptation. *Zoological Lett.* **4**, 10 (2018).
84. H. M. Dunsworth, A. G. Warrener, T. Deacon, P. T. Ellison, H. Pontzer, Metabolic hypothesis for human altriciality. *Proc. Natl. Acad. Sci. U.S.A.* **109**, 15212–15216 (2012).
85. K. Rosenberg, W. Trevathan, Bipedalism and human birth: The obstetrical dilemma revisited. *Evol. Anthropol: Issues News Rev.* **4**, 161–168 (1995).
86. B. Bogin, *Patterns of Human Growth* (Cambridge University Press, ed. 2, 1999).
87. A. Portmann, *A Zoologist Looks at Humankind* (Schwabe, 1969).
88. B. Wood, Reconstructing human evolution: Achievements, challenges, and opportunities. *Proc. Natl. Acad. Sci. U.S.A.* **107**, 8902–8909 (2010).
89. B. Bogin, The evolution of human childhood. *Bioscience* **40**, 16–25 (1990).
90. J. L. Locke, B. Bogin, Life history and language: Selection in development. *Behav. Brain Sci.* **29**, 301–311 (2006).
91. D. I. Anderson *et al.*, The role of locomotion in psychological development. *Front. Psychol.* **4**, 1–17 (2013).
92. J. J. Campos *et al.*, Travel broadens the mind. *Infancy* **1**, 149–219 (2000).
93. A. Dahl *et al.*, The epigenesis of wariness of heights. *Psychol. Sci.* **24**, 1361–1367 (2013).
94. I. Uchiyama *et al.*, Locomotor experience affects self and emotion. *Dev. Psychol.* **44**, 1225–1231 (2008).
95. A. L. Zihlman, Locomotion as a life history character: The contribution of anatomy. *J. Hum. Evol.* **22**, 315–325 (1992).
96. A. le Cabec, N. Tang, P. Tafforeau, Accessing developmental information of fossil hominin teeth using new synchrotron microtomography-based visualization techniques of dental surfaces and interfaces. *PLoS One* **10**, e0123019 (2015).
97. M. C. Dean, Retrieving chronological age from dental remains of early fossil hominins to reconstruct human growth in the past. *Philos. Trans. R. Soc. B Biol. Sci.* **365**, 3397–3410 (2010).
98. D. R. Bolter, M. C. Elliott, J. Hawks, L. R. Berger, Immature remains and the first partial skeleton of a juvenile Homo naledi, a late middle pleistocene hominin from South Africa. *PLoS One* **15**, e0230440 (2020).
99. L. J. D. DeMars *et al.*, Using point clouds to investigate the relationship between trabecular bone phenotype and behavior: An example utilizing the human calcaneus. *Am. J. Hum. Biol.* **33**, e23468 (2021).
100. T. Torigoe, Development of posture and locomotion in Japanese monkey infants. *Annu. Animal Psychol.* **34**, 11–18 (1984).
101. H. B. Smith, T. L. Crummett, K. L. Brandt, Ages of eruption of primate teeth: A compendium for aging individuals and comparing life histories. *Am. J. Phys. Anthropol.* **37**, 177–231 (1994).
102. M. C. Dean, B. A. Wood, Developing Pongid Dentition and it's use for ageing individual crania in comparative cross-sectional growth studies. *Folia Primatol.* **36**, 111–127 (1981).
103. L. Scheuer, S. M. Black, *The Juvenile Skeleton*, E. A. Press, Ed. (Academic Press, 2004).
104. C. B. Ruff, Body size prediction from juvenile skeletal remains. *Am. J. Phys. Anthropol.* **188**, 698–716 (2007).
105. N. Van Minh, Y. Hamada, Age-related changes of sulcal imprints on the endocranium in the Japanese macaque (Macaca fuscata). *Am. J. Phys. Anthropol.* **163**, 285–294 (2017).
106. J. M. DeSilva, J. J. Lesnik, Brain size at birth throughout human evolution: A new method for estimating neonatal brain size in hominins. *J. Hum. Evol.* **55**, 1064–1074 (2008).
107. Z. Cofran, J. M. Desilva, A neonatal perspective on Homo erectus brain growth. *J. Hum. Evol.* **81**, 41–47 (2015).
108. C. A. Schneider, W. S. Rasband, K. W. Eliceiri, NIH image to ImageJ: 25 years of image analysis. *Nat. Methods* **9**, 671–675 (2012).
109. N. Reznikov, H. Liang, M. D. McKee, N. Piché, Technical note: Mapping of trabecular bone anisotropy and volume fraction in 3D using μCT images of the human calcaneus. *Am. J. Biol. Anthropol.* **177**, 566–580 (2022).
110. T. Kohler, M. Stauber, L. R. Donahue, R. Müller, Automated compartmental analysis for high-throughput skeletal phenotyping in femora of genetic mouse models. *Bone* **41**, 659–667 (2007).
111. D. P. Fyhrie, D. R. Carter, A unifying principle relating stress to trabecular bone morphology. *J. Orthop. Res.* **4**, 304–317 (1986).
112. D. R. Carter, D. P. Fyhrie, R. T. Whales, Trabecular bone density and loading history: Regulation of connective tissue biology by mechanical energy. *J. Biomech.* **20**, 785–794 (1987).
113. V. L. Giddings, G. S. Beaupré, R. T. Whalen, D. R. Carter, Calcaneal loading during walking and running. *Med. Sci. Sports Excerc.* **32**, 627–634 (2000).
114. D. A. Winter, *Biomechanics and Motor Control of Human Movement* (Wiley, 2009).
115. B. Demes *et al.*, The kinetics of primate quadrupedalism: "Hindlimb drive" reconsidered. *J. Hum. Evol.* **26**, 353–374 (1994).
116. H. Pontzer, D. A. Raichlen, P. S. Rodman, Bipedal and quadrupedal locomotion in chimpanzees. *J. Hum. Evol.* **66**, 64–82 (2014).
117. V. Camomilla *et al.*, Methodological factors affecting joint moments estimation in clinical gait analysis: A systematic review. *Biomed. Eng. Online* **16**, 106 (2017).
118. H. Akaike, A new look at the statistical model identification. *IEEE Trans. Automat. Contr.* **19**, 716–723 (1974).
119. R. McElreath, *Statistical Rethinking: A Bayesian Course with Examples in R and Stan* (Chapman and Hall/CRC, 2015), 10.3102/1076998616659752.
120. V. M. Muggeo, Segmented: An R package to fit regression models with broken-line relationships. *R News* **8**, 20–25 (2008).